16. Mantsch P (for the Pierre Auger Collab.) "The Pierre Auger Observatory progress and first results", astro-ph/0604114
17. Tokuno H et al. *AIP Conf. Proc.* **1238** 365 (2010)
18. Boldt E, Ghosh P *Mon. Not. R. Astron. Soc.* **307** 491 (1999); astro-ph/9902342
19. Neronov A, Tinyakov P, Tkachev I *Zh. Eksp. Teor. Fiz.* **127** 744 (2005) [*JETP* **100** 656 (2005)]; astro-ph/0402132
20. Berezinsky V, Kachelrieß M, Vilenkin A *Phys. Rev. Lett.* **79** 4302 (1997); astro-ph/9708217
21. Kuzmin V A, Rubakov V A *Yad. Fiz.* **61** 1122 (1998) [*Phys. At. Nucl.* **61** 1028 (1998); astro-ph/9709187
22. Chung D J H, Kolb E W, Riotto A *Phys. Rev. D* **59** 023501 (1999)
23. Kuzmin V A, Tkachev I I *Pis'ma Zh. Eksp. Teor. Fiz.* **68** 255 (2005) [*JETP Lett.* **68** 271 (1998)]
24. Kuzmin V, Tkachev I *Phys. Rev. D* **59** 123006 (1999)
25. Dubovsky S L, Tinyakov P G *Pis'ma Zh. Eksp. Teor. Fiz.* **68** 99 (1998) [*JETP Lett.* **68** 107 (1998); hep-ph/9802382
26. Berezinsky V, Mikhailov A A *Phys. Lett. B* **449** 237 (1999); astro-ph/9810277
27. Chung D J H, Farrar G R, Kolb E W *Phys. Rev. D* **57** 4606 (1998); astro-ph/9707036
28. Berezinsky V, Kachelrieß M, Ostapchenko S *Phys. Rev. D* **65** 083004 (2002); astro-ph/0109026
29. Gorbunov D S, Raffelt G G, Semikoz D V *Phys. Rev. D* **64** 096005 (2001); hep-ph/0103175
30. Csáki C et al. *JCAP* (05) 005 (2003); hep-ph/0302030
31. Fairbairn M, Rashba T, Troitsky S V, arXiv:0901.4085
32. Coleman S, Glashow S L *Phys. Rev. D* **59** 116008 (1999); hep-ph/9812418
33. Dubovsky S L, Tinyakov P G *Astropart. Phys.* **18** 89 (2002); astro-ph/0106472
34. Berezinsky V, Gazizov A Z, Grigorieva S I *Phys. Lett. B* **612** 147 (2005); astro-ph/0502550
35. Stokes B et al. (for the Telescope Array Collab.), in *Proc. of the Intern. Symp. on the Recent Progress of Ultra-High Energy Cosmic Ray Observation*: *UHECR, Nagoya, Japan, December 10–12, 2010*
36. Abbasi R U et al. (HiRes Collab.) *Phys. Rev. Lett.* **100** 101101 (2008); astro-ph/0703099
37. Abraham J et al. (Pierre Auger Collab.) *Phys. Rev. Lett.* **101** 061101 (2008); arXiv:0806.4302
38. Kalashev O E, Rubtsov G I, Troitsky S V *Phys. Rev. D* **80** 103006 (2009); arXiv:0812.1020
39. Rodriguez D C, Ph.D. Thesis (Salt Lake City, UT: Univ. of Utah, 2011)
40. Ikeda D et al. (for the Telescope Array Collab.), in *Proc. of the Intern. Symp. on the Recent Progress of Ultra-High Energy Cosmic Ray Observation*: *UHECR, Nagoya, Japan, December 10–12, 2010*
41. Abbasi R U et al. (HiRes Collab.) *Phys. Rev. Lett.* **104** 161101 (2010); arXiv:0910.4184
42. Abraham J et al. (Pierre Auger Collab.) *Phys. Rev. Lett.* **104** 091101 (2010); arXiv:1002.0699
43. Tameda Y et al. (for the Telescope Array Collab.), in *Proc. of the Intern. Symp. on the Recent Progress of Ultra-High Energy Cosmic Ray Observation*: *UHECR, Nagoya, Japan, December 10–12, 2010*
44. Rubtsov G I et al. (for the Telescope Array Collab.), in *Proc. of the Intern. Symp. on the Recent Progress of Ultra-High Energy Cosmic Ray Observation*: *UHECR, Nagoya, Japan, December 10–12, 2010*
45. Glushkov A V et al. *Pis'ma Zh. Eksp. Teor. Fiz.* **85** 163 (2007) [*JETP Lett.* **85** 131 (2007)]; astro-ph/0701245
46. Gorbunov D S, Rubtsov G I, Troitsky S V *Astropart. Phys.* **28** 28 (2007); astro-ph/0606442
47. Tinyakov P et al. (for the Telescope Array Collab.), in *Proc. of the Intern. Symp. on the Recent Progress of Ultra-High Energy Cosmic Ray Observation*: *UHECR, Nagoya, Japan, December 10–12, 2010*
48. Hayashida N et al. *Phys. Rev. Lett.* **77** 1000 (1996)
49. Tinyakov P G, Tkachev I I *Pis'ma Zh. Eksp. Teor. Fiz.* **74** 3 (2001) [*JETP Lett.* **74** 1 (2001)]; astro-ph/0102101
50. Abraham J et al. (Pierre Auger Collab.) *Science* **318** 938 (2007); arXiv:0711.2256
51. Veron-Cetty M P, Veron P "Quasars and active galactic nuclei", ESO Scientific Report 19, 9th ed. (2000)
52. Koers H B J, Tinyakov P *JCAP* (04) 003 (2009); arXiv:0812.0860
53. Abbasi R U et al., arXiv:1002.1444

PACS numbers: 14.60.Pq, 25.30.Pt
DOI: 10.3367/UFNe.0181.201109j.0997

T2K neutrino experiment: first results

Yu G Kudenko

1. Introduction

The discovery of neutrino oscillations became direct experimental evidence of the existence of new physics beyond the framework of the Standard Model and simultaneously marked the beginning of the study of this physics. As follows from the oscillations, neutrinos possess a small nonzero mass, they mix, and neutrino flavors (lepton numbers) are not conserved. Neutrino oscillations are described by the so-called neutrino Standard Model (νSM), which is the minimal model describing the mixing of three neutrino types. The physics of neutrino oscillations is described by a unitary matrix U [1] that relates three types of active neutrinos with left-handed helicity, ν_e, ν_μ, and ν_τ, to the mass eigenstates ν_1, ν_2, and ν_3 with the respective masses m_1, m_2, and m_3. In a form convenient for physical analysis, the matrix U can be represented as follows:

$$U=\begin{pmatrix}1 & 0 & 0\\ 0 & c_{23} & s_{23}\\ 0 & -s_{23} & c_{23}\end{pmatrix}\begin{pmatrix}c_{13} & 0 & s_{13}\exp(-\mathrm{i}\delta)\\ 0 & 1 & 0\\ -s_{13}\exp(\mathrm{i}\delta) & 0 & c_{13}\end{pmatrix}\times\begin{pmatrix}c_{12} & s_{12} & 0\\ -s_{12} & c_{12} & 0\\ 0 & 0 & 1\end{pmatrix}. \quad (1)$$

In this expression, $s_{ij}\equiv\sin\theta_{ij}$ and $c_{ij}\equiv\cos\theta_{ij}$ $(i,j=1,2,3)$. Neutrino oscillations are described by six parameters: two independent mass squared differences: $\Delta m_{12}^2=m_2^2-m_1^2$ and $\Delta m_{23}^2=m_3^2-m_2^2$; three mixing angles: θ_{12}, θ_{23}, θ_{13}, and a CP-odd phase δ.

Experiments with atmospheric [2], solar [3–8], reactor [9], and accelerator [10, 11] neutrinos measured four parameters θ_{12}, θ_{23}, Δm_{12}^2, and Δm_{23}^2: $\tan^2\theta_{12}=0.47^{+0.06}_{-0.05}$, $\Delta m_{12}^2=7.59^{+0.21}_{-0.21}\times10^{-5}$ eV^2, $\sin^2 2\theta_{23}>0.92$ for a 90-percent confidence interval (90% CL), and $\Delta m_{23}^2=(2.43\pm0.13)\times10^{-3}$ eV^2. It is pertinent to note that the sign of Δm_{23}^2 is unknown, i.e., the neutrino mass hierarchy has not been determined. Both the normal hierarchy, $m_3\gg m_2>m_1$, and inverse hierarchy, $m_2>m_1\gg m_3$, are possible. Furthermore, the parameters θ_{13} and δ have not been measured. The best limit, $\sin^2 2\theta_{13}<0.15$ (90% CL) for $\Delta m_{23}^2=2.43\times10^{-3}$ eV^2, was obtained in the ChOOZ experiment [12].

Since $|\Delta m_{12}^2|\ll|\Delta m_{13}^2|\simeq|\Delta m_{23}^2|$ and the typical baselines of accelerator experiments for studying neutrino oscillations in the region of 'atmospheric' parameters ($\Delta m_{23}^2\sim(2-3)\times10^{-3}$ eV^2) amount to several hundred kilometers, the contribution of Δm_{12}^2-bearing terms to the oscillation probability is small, so that approximate expressions for muon neutrino

Yu G Kudenko Institute for Nuclear Research,
Russian Academy of Sciences, Moscow, Russian Federation
E-mail: kudenko@inr.ru

Uspekhi Fizicheskikh Nauk **181** (9) 997–1004 (2011)
DOI: 10.3367/UFNr.0181.201109j.0997
Translated by E N Ragozin; edited by A Radzig

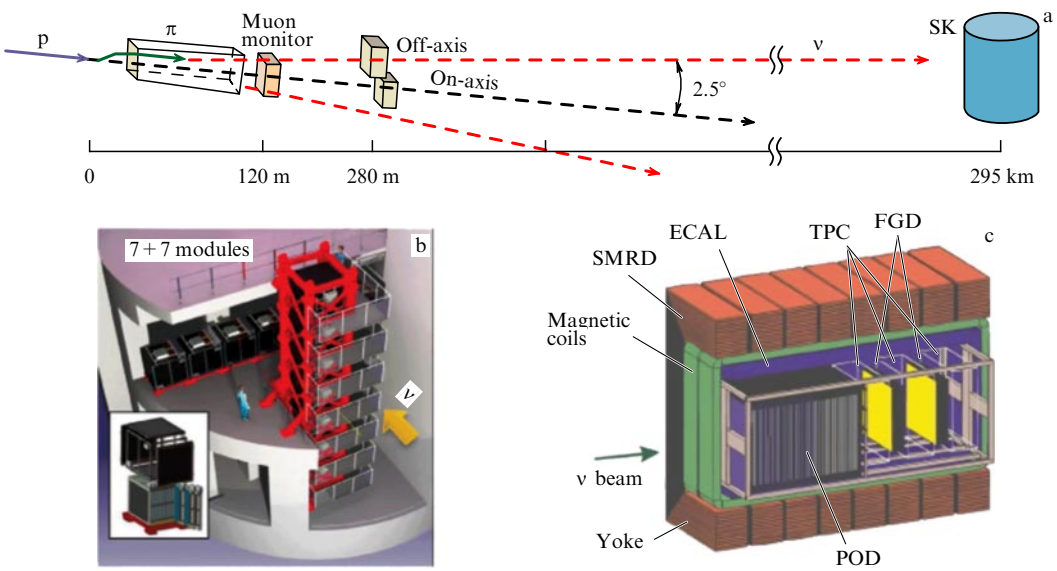

Figure 1. Layout of the T2K experiment: (a) main elements of the facility — neutrino beam, neutrino beam monitor, ND280 near neutrino detector located 280 m away from the target, and Super-Kamiokande far neutrino detector (SK); (b) general view of the INGRID on-axis neutrino beam monitor, and (c) near off-axis neutrino detector, which comprises a neutral-pion detector (POD), an electromagnetic calorimeter (ECAL), a side muon range detector (SMRD), and a tracking detector, which consists of three time-projection chambers (TPCs) and two (scintillation) fine-grained detectors (FGDs).

oscillations may be written in the following form [13, 14]:

$$P(\nu_\mu \to \nu_e) \simeq \sin^2 2\theta_{13} \sin^2 \theta_{23} \sin^2 \frac{\Delta m^2_{13} L}{4E_\nu}\,, \tag{2}$$

$$P(\nu_\mu \to \nu_\mu) \simeq 1 - \sin^2 2\theta_{23} \cos^4 \theta_{13} \sin^2 \frac{\Delta m^2_{13} L}{4E_\nu} - P(\nu_\mu \to \nu_e)\,. \tag{3}$$

When the neutrino energy and the experiment baseline are selected in such a way that the oscillation probability $P(\nu_\mu \to \nu_e)$ is at its maximum, i.e. $(\Delta m^2_{13} L)/(4E_\nu) = \pi/2 + n\pi$, then

$$P(\nu_\mu \to \nu_e) \approx \frac{1}{2} \sin^2 2\theta_{13}\,. \tag{4}$$

The primary goal of the T2K (Tokai-to-Kamioka) second-generation long-baseline experiment [15] performed in Japan is the quest for $\nu_\mu \to \nu_e$ oscillations and the measurement of the θ_{13} angle with a sensitivity of up to $\sin^2 2\theta_{13} \sim 0.006$ (90% CL), and precision measurements of other oscillation parameters with an accuracy of $\delta(\sin^2 2\theta_{23}) \sim 0.01$ and $\delta(\Delta m^2_{23}) \sim 10^{-4}$ eV^2. More than 500 scientists from 12 countries are members of the T2K collaboration. Participating in the experiment on the part of Russia is the Institute for Nuclear Research (INR), Russian Academy of Sciences. The conception of this experiment, the experimental facility, first results, its status, and short-term prospects are outlined below.

2. T2K experimental facility

The general layout of the experiment is shown in Fig. 1. The main elements of the facility are the neutrino channel, the array of near neutrino detectors (ND280) located 280 m away from the target, and the far Super-Kamiokande detector (SK) located 295 km from the target. The near detector ND280 [16–18] consists of two neutrino detectors stationed in a 40-m-deep pit about 18 m in diameter. It is employed for measuring the parameters of the neutrino beam near the target (prior to oscillations), monitoring its properties, and measuring the neutrino–nuclei interaction cross sections. One detector [the neutrino beam monitor INGRID (Interactive Neutrino GRID)] is located on the beam axis, i.e., at a zero angle to the direction of the proton beam, and the other (off-axis) near neutrino detector is located on the axis connecting the decay volume and Super-Kamiokande detector, i.e., at an angle of 2.5°.

2.1 Neutrino beam

For the first time, the T2K experiment uses a quasimonoenergetic off-axis neutrino beam whose energy is tuned to the first oscillation maximum. As follows from the $\pi \to \mu + \nu$ decay kinematics, the neutrino energy E_ν depends only slightly on the pion energy E_π for a small angle θ between the pion and neutrino momenta. This off-axis muon-neutrino beam concept was implemented at the 30-GeV high-current proton synchrotron Japan Proton Accelerator Research Complex (J-PARC). The accelerator power is designed to be 0.75 MW, which affords a proton beam intensity of 3.3×10^{14} protons per pulse for a pulse duration of about 3.0 μs and a fast beam extraction and its delivery to the target every 3.2 s. The experiment uses a graphite target 30 mm in diameter and 900 mm in length (≈ 2 nuclear lengths), in which about 80% of the protons participate in nuclear interactions. The target is cooled by gaseous helium. Three toroidal pulsed magnets focus the generated pions into the 94-m-long decay volume which is filled with helium at a pressure of 1 atm to reduce pion absorption and production.

The spectra of muon neutrinos calculated for several θ angles are displayed in Fig. 2. The basic version of the experiment corresponds to the angle of 2.5° that can be varied between 2.0° and 3.0°, which allows changing the average neutrino energy from 0.5 to 0.9 GeV and optimizing the experimental sensitivity to the oscillation parameters [19, 20]. For neutrino energies corresponding to the intensity

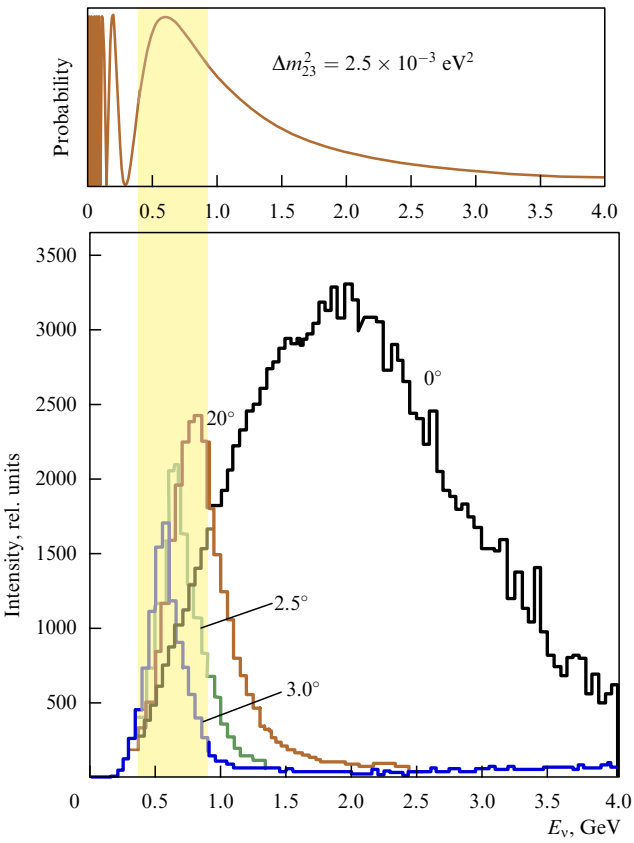

Figure 2. Neutrino spectra for different angles relative to the proton beam axis: 0°, 2.0°, 2.5°, and 3.0°. The T2K experiment uses the beam at an angle of 2.5°, tuned to the first oscillation maximum for $\Delta m^2_{23} = 2.5 \times 10^{-3}$ eV^2, as is evident from the oscillation probability curve depicted in the upper part of the figure.

maximum, the admixture of electron neutrinos from the $\pi \to \mu \to e$ decay chain and the decay of kaons is about 0.4% for the angle of 2.5°. It is noteworthy that the off-axis neutrino beam parameters, which depend strongly on the angle, as is clear from Fig. 2, should be carefully monitored in the course of the experiment.

2.2 Near neutrino detector

To achieve the main experiment goals, the near neutrino detector must provide the measurement of the neutrino energy spectrum near the target with an accuracy of 2%. To obtain the neutrino energy with this accuracy, the spectrum of muons from the quasielastic neutrino scattering should be measured with a momentum resolution $\Delta p/p \leqslant 10\%$, and the absolute value of the muon momentum should be determined with a precision better than 2%. Furthermore, the detector should have a low proton detection threshold (≈ 200 MeV/c). The admixture of electron neutrinos to the muon neutrino spectrum has to be measured with an accuracy of $\approx 10\%$. One of the main detector tasks also involves the measurement of neutrino scattering cross sections on nucleons and light nuclei for neutrino energies from 500 to 1500 MeV. The principal function of the neutrino beam monitor consists in measuring the beam profile and monitoring the direction of the neutrino beam with an uncertainty of less than 1 mrad, which ensures monitoring the neutrino energy in the SK direction to better than 15 MeV at the maximum of the spectrum.

Neutrino beam monitor. The monitor of the neutrino beam, the Interactive Neutrino GRID (INGRID), consists of 7 + 7 identical modules arranged in the form of a cross, and two additional modules, as shown in Fig. 1b. Each module of lateral size 1×1 m^2 has a steel–scintillator sandwich structure and consists of 10 alternating steel layers 6.5 cm thick and of 11 scintillating planes. The active plane is made up of two scintillating layers, each being an assembly of scintillating bars which are arranged vertically in one layer and horizontally in the other. A wavelength-shifting fiber transmits the scintillation signal to a photodetector Multi-Pixel Photon Counter (MPPC) developed by Hamamatsu, Japan, which is made up of multiple avalanche photodiode pixels operating in the limited Geiger mode. A description of these devices, their parameters, and the test data are given in Refs [21–24]. The total weight of the monitor is about 160 t.

Off-axis detector. The near (off-axis) neutrino detector is composed of a UA1 magnet which houses a pi zero detector (π^0 detector, or P0D), a tracking detector which comprises three time projection chambers (TPCs) and two highly segmented scintillation detectors (fine-grained detectors, or FGDs), an electromagnetic calorimeter (ECAL), and a side muon range detector (SMRD), as shown in Fig. 1c. With the exception of the TPCs, scintillation detectors with wavelength-shifting fibers are used for active elements in all of these detectors, with MPPCs serving as photodetectors. The pi zero detector is optimized for measuring the π^0 production cross section via neutral currents:

$$\nu_\mu + N \to \nu_\mu + \pi^0 + N\,, \tag{5}$$

where $N = \mathrm{n}, \mathrm{p}$. Measuring these processes plays an important role in determining the level of the physical background in the spectrum of electron neutrinos emerging in Super-Kamiokande due to $\nu_\mu \to \nu_e$ oscillations (if $\theta_{13} \neq 0$), because an event in which only one photon from the $\pi^0 \to \gamma\gamma$ decay is detected is identified as a single electron from the quasielastic scattering of an electron neutrino. The P0D consists of alternating water layers, each 3 cm thick, and tracking planes. One tracking plane, in turn, consists of two XY planes, in which scintillating bars are arranged perpendicular to each other. For the efficient detection of photons, thin brass foils are placed between the scintillating bars in the central part of the detector, and lead plates are inserted in the front and rear parts of the detector. The total P0D weight is about 17 t, and the water target weight is about 3 t. Since the active element of the far detector comprises water, reducing systematic errors calls for measurements of the cross section for neutral pion production on oxygen for neutrino energies less than 1 GeV. The P0D will also be employed for solving this problem.

The tracking detector measures the flux and spectrum of muon and electron neutrinos by detecting charged leptons produced in the quasielastic neutrino scattering. The principal muon neutrino–nucleon interaction process for T2K energies is the quasielastic scattering via charged current:

$$\nu_\mu + \mathrm{n} \to \mu^- + \mathrm{p}\,. \tag{6}$$

Precisely measuring the neutrino spectrum requires detecting and reconstructing the kinematic parameters of both the muon and the proton. The proton is identified and measured by the FGDs, and the muon momentum is measured by the TPC with the addition of information provided by FGDs.

The first FGD is a full-active scintillation detector consisting of 30 layers of scintillating bars with the 1×1 cm^2 cross section, which form alternating XY layers perpendicular to the neutrino beam direction. The second FGD contains 3-cm-thick water layers between scintillating layers. The total water weight is 0.44 t. This configuration allows simultaneously measuring the cross sections for neutrino interactions in water and carbon by comparing the events occurring in both detectors.

Three time-projection chambers, which are embedded in a 0.2-T magnetic field, should provide a momentum resolution of about 10% in the 1-GeV/c muon momentum range. High resolution ($< 10\%$) was also achieved in measuring the specific energy loss $\mathrm{d}E/\mathrm{d}x$, which will enable a reliable (at a level of 5σ) identification of muons and electrons in the 0.3–1.0 GeV/c momentum range.

The tracking detectors and the P0D are surrounded by an electromagnetic calorimeter whose primary function lies in the detection and identification of the particles that escape from the volume of these detectors. The calorimeter, which has an effective thickness of about 10 radiation lengths, consists of alternating layers of lead and plastic scintillator, and exhibits an energy resolution of $7.5\%/\sqrt{E\,[\mathrm{GeV}]}$ for electromagnetic showers. The muons escaping from the tracking detector at large angles cannot be measured by the TPC. They enter the magnet yoke and their momentum can be measured from their range determined using the SMRD, which was developed and built at INR, RAS. The active elements of this detector are 2100 scintillation detectors [25, 26] located in the air gaps between magnet sections.

The near neutrino detector thus configured permits measuring the neutrino beam near the target (the spectrum and the intensity at the angles of 0° and 2.5°), the admixture of electron neutrinos that arise from the decays of muons and kaons, and the cross sections of neutrino interactions with nucleons and different nuclei via charged and neutral currents. Based on these measurements, predictions for the spectrum and number of muon and electron neutrinos in the SK far detector in the absence of oscillations are made.

2.3 Super-Kamiokande far detector

The Super-Kamiokande facility [27], which is a water Cherenkov detector 50,000 m^3 in volume, is located near Kamioka, Japan in a disused Mozumi mine under Mount Kamioka. Because the thickness of the rock is about 1 km, which corresponds to 2700 m of water equivalent, cosmic muons with energies below 1.3 TeV do not reach the detector, and the high-energy muon flux is suppressed by a factor of about 10^6.

The detector, a giant tank 39 m in diameter and 42 m in height filled with ultrapure water, consists of two detectors: an inner one, and an outer one. The entire volume of the inner detector is viewed by approximately eleven thousand spherical photomultiplier tubes (PMTs), with a 1–300 photoelectron dynamic range. The PMTs are arranged in a 70-cm pitch array on the walls, top, and bottom of the detector. The photocathode of each PMT measures 50 cm in diameter; the total photocathode area, i.e., the active part of the photomultiplier tubes, covers 40% of the entire detector surface. The optically isolated water volume with a weight of 18 kt surrounding the inner detector is viewed by 1885 PMTs 20 cm in diameter (the outer detector). In this detector, the average water layer thickness is equal to 2.7 m. The outer detector operates as an active 4π-veto-detector for charged particles and also serves as a passive shield from the neutrons and gamma-ray photons from the mountain rock. The water transparency in the detector is about 100 m for Cherenkov radiation at a wavelength of 420 nm.

The Super-Kamiokande detects neutrinos in the energy range from 4.5 MeV to 1 TeV. For low-energy events (primarily for the study of solar neutrinos), the energy of a charged particle is determined using the number of PMT hits, while high-energy events are measured from the total number of photoelectrons of all the PMTs actuated.

The dimension, shape, and direction of the Cherenkov cone are used for event identification: a single-ring muon-like, single-ring e-like, or multiple-ring event. The momentum resolution of the detector amounts to 2.4% for muons with a momentum of 1 GeV/c. The time synchronization between the pulse of the J-PARC proton accelerator and Super-Kamiokande was provided via the Global Positioning System (GPS) with a precision of 50 ns. This precision allows observing the beam microstructure in the neutrino events detected by the SK and enables suppressing the atmospheric neutrino background to a negligible level.

3. Status of the T2K experiment and preliminary results

The construction of the J-PARC accelerator complex was completed in 2008. In April 2009, the proton beam was injected into the neutrino channel and the muon monitor detected the muon signal from the $\pi^+ \to \mu^+ + \nu$ decay. In November 2009, the first neutrino events were recorded by the ND280 near detector, all of whose elements had been practically installed by that time. The accumulation of statistics commenced in January 2010, and the first neutrino event in Super-Kamiokande was detected in February 2010. The integral number of protons accumulated on the target during the first run (January–June 2010) amounted to 3.3×10^{19} at an average proton beam power of ≈ 50 kW. The operation efficiencies of Super-Kamiokande and ND280 detectors during data taking period exceeded 99% and 96%, respectively. The preliminary results of the first physical run are outlined below.

3.1 Neutrino beam properties

The near detector measured and monitored the initial neutrino beam parameters near the decay volume, i.e., prior to possible oscillations. The profile of the neutrino beam and its direction relative to the proton beam axis (0°) are measured by the INGRID detector. To this end, use is made of the reaction of the quasielastic muon neutrino scattering (6). The measured neutrino beam profile is plotted in Fig. 3a, and the position of the beam center during the accumulation of statistics for about a month is shown in Fig. 3b. The position of the beam center is stable within the range required, ± 1 mrad (± 28.5 cm). A graphic representation of the first neutrino event in the ND280 near detector in the Super-Kamiokande direction (2.5°) is given in Fig. 4a: a muon track arising from a neutrino interaction in the P0D was reconstructed in three TPCs and both FGDs. The time structure of neutrino events in the SMRD shown in Fig. 4d is in complete agreement with the structure of the proton beam in the first physics run, which had six microbunches spaced by 580 ns.

It is noteworthy that the events between microbunches are practically lacking, which testifies to a very good proton-

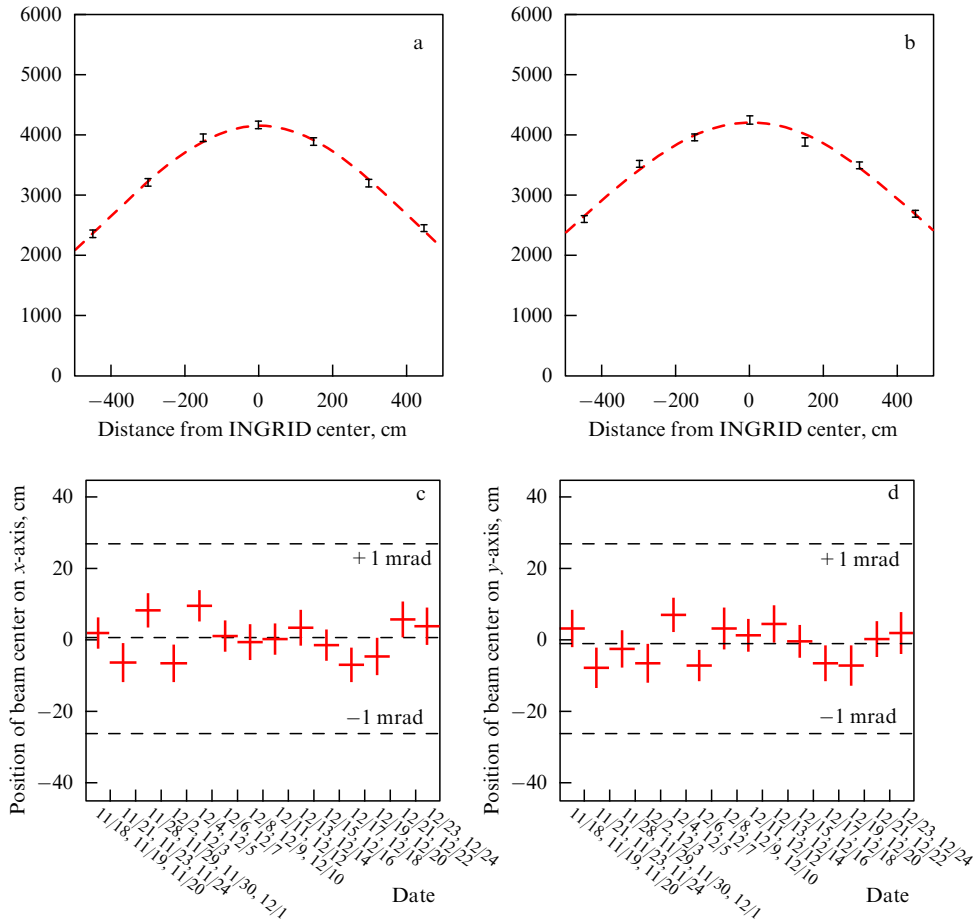

Figure 3. Neutrino beam measured by INGRID at an angle of 0°: horizontal (a) and vertical (b) profiles of the neutrino beam; horizontal (c) and vertical (d) position of the beam center over several months of measurements in 2010. Horizontal dashed lines indicate the admissible interval for beam center deviations, ±1 mrad, from the direction of the proton beam (0°).

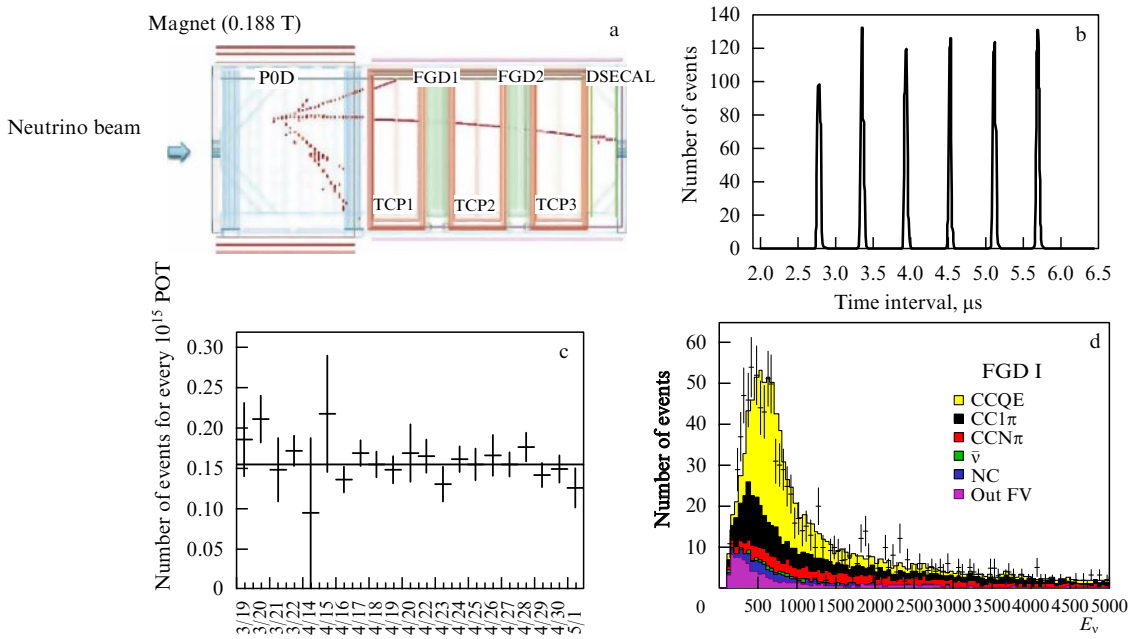

Figure 4. Neutrino events in the ND280 near detector. (a) The first neutrino event detected in the near detector. (b) Time distribution of neutrino events in SMRD: 6 peaks, which are spaced by 580 ns, correspond to 6 proton beam microbunches in the first physics run in 2010. (c) The number of neutrino events in FGD normalized to 10^{15} protons on target in 2010. (d) Neutrino spectrum in the near detector reconstructed from the neutrino events detected by FGD1; also shown are the spectra of different processes obtained by Monte Carlo simulations. Most important processes among them are quasielastic scattering (shown in yellow) and inelastic scattering with the production of a single pion (black). (See in color at www.ufn.ru.)

beam modulation structure without protons between the microbunches, and to a very low background level in ND280.

The number of neutrino events recorded in the near detector (FGD) for every 10^{15} protons on target (POT) is presented in Fig. 4c, which makes evident the good stability of detection of neutrino events over the period of accelerator operation. Figure 4d demonstrates the spectrum of muon neutrinos reconstructed from the events detected by FGD1. Also shown here are the characteristics of the main processes contributing to this spectrum, which were obtained by the Monte Carlo method. As is clear from this figure, the measured and calculated spectra of neutrinos near the target are in rather good agreement. A small excess of experimental events is seen at low energies, 350–2500 MeV, which is most likely attributable to the detection of secondary particles from neutrino events in the magnet and pit walls, which have yet to be completely included in the simulations. Of special note is the fact that the maximum of the spectrum falls in the 600–700 MeV neutrino energy range, i.e., the neutrino beam is tuned to the oscillation maximum, as initially planned in the design of the neutrino channel and off-axis angle selection.

3.2 Oscillation analysis

The first stage of the experiment is aimed at solving two main problems: precision measurements of $\nu_\mu \to \nu_\mu$ oscillation parameters, and the quest for the $\nu_\mu \to \nu_e$ transition and measurement of the θ_{13} angle.

3.2.1 $\nu_\mu \to \nu_\mu$. The basic process whereby muon neutrinos are detected at an energy of ≈ 700 MeV is their quasielastic scattering via charged current [see expression (6)]. Super-Kamiokande detects a muon and measures its energy with a resolution of about 2.5%, and the direction of its momentum with an angular resolution of about 1°. In this case, the uncertainty in determining the absolute value of the muon energy, i.e., the uncertainty in the energy scale of the detector, amounts to only about 2%. The expected neutrino flux $\Phi_{\rm SK}^{\rm expect}$ in Super-Kamiokande (without oscillations) is simulated by the Monte Carlo technique with the use of the initial flux $\Phi_{\rm ND}$ and neutrino spectrum near the decay volume measured in ND280:

$$\Phi_{\rm SK}^{\rm expect} = R_{\rm F/N}\,\Phi_{\rm ND}\,, \tag{7}$$

where $R_{\rm F/N}$ is the ratio between the neutrino fluxes in the far (F) and near (N) detectors. To minimize the uncertainties arising from the model description of hadron production processes, $R_{\rm F/N}$ simulations are performed with the use of the information about experimental cross sections of hadron production in proton-nuclear interactions measured with a graphite target, which is a copy of the T2K target, in the NA61 experiment at CERN [28]. The neutrino flux in the near detector is defined as follows:

$$\Phi_{\rm ND} = \frac{N_{\rm ND}^{\rm obs}}{\sigma_{\rm ND}\,\epsilon_{\rm ND}}\,, \tag{8}$$

where $N_{\rm ND}^{\rm obs}$ is the measured number of neutrino events in the near detector, and $\sigma_{\rm ND}$ and $\epsilon_{\rm ND}$ are the cross section of muon neutrino interaction and the efficiency of muon neutrino detection in ND280, respectively. Oscillation parameters (Δm_{23}^2 and $\sin^2 2\theta_{23}$) are obtained from the fitting of the measured spectrum and the number of neutrino events using expression (3).

Criteria for the selection of events were fixed beforehand on the basis of the simulations of neutrino processes at Super-Kamiokande, and they also relied on the techniques elaborated for the data analysis of K2K and Super-Kamiokande experiments. These criteria were as follows: (i) timing correlation with the J-PARC beam taking into consideration the time of flight to Super-Kamiokande correct to within ≈ 50 ns; (ii) the energy of a neutrino event is completely absorbed by the inner detector (the absence of any signal in the outer detector); (iii) the vertex of neutrino interaction is more than 2 m away from the walls of the inner detector; (iv) the number of rings is equal to unity; (v) the detected event energy > 100 MeV, and (vi) the ring should be muon-like. A typical muon-like ring is depicted in Fig. 5a.

As a result of the first physics run with 3.3×10^{19} POT, 33 muon neutrinos produced in the sensitive detector volume were detected at Super-Kamiokande; their energy was completely deposited in the inner detector. On the other hand, 49.5 events were expected for the same number of protons in the absence of oscillations.

Therefore, an event deficit typical of oscillations was observed, although the statistics are still poor. That these are accelerator neutrinos is confirmed by the temporal structure of these events, which is in perfect agreement with the proton beam structure, as seen from Fig. 5b. Special mention should be made of the absence of background prior to, after, and between microbunches, as well as of the high temporal resolution of the entire facility: $\sigma \approx 26$ ns (Fig. 5d). The background expected in the first session was about 0.01 events, i.e., it was negligible. The application of the Kolmogorov–Smirnov criterion for testing the correspondence between the event detection at Super-Kamiokande and the number of protons on target reveals that the probability of corresponding the distribution depicted in Fig. 5a to the expected linear dependence is equal to 8%.

3.2.2 $\nu_\mu \to \nu_e$. To measure the characteristics of this process and, in particular, determine the mixing angle θ_{13}, it is necessary to efficiently detect the electrons emerging in Super-Kamiokande as a result of the interaction of electron neutrinos with nucleons via charged currents, as well as to efficiently suppress those events in which neutral pions are produced via neutral currents. The problem consists in π^0 identification in the case of asymmetric $\pi^0 \to \gamma\gamma$ decay, when one of the photons has a low energy, resulting in the actuation of a small number of PMTs at Super-Kamiokande, with the identification of the Cherenkov ring of this photon being hindered.

To detect an electron from an electron neutrino, the of selection criteria 1–4 listed in Section 3.2.1 are applied using the following conditions: the detected event energy exceeds 30 MeV; the ring is electron-like, and there is no delayed electron signal from the decay of a muon produced in the course of neutrino interactions.

The last condition is applied to eliminate events in which a muon-like ring satisfies the selection criteria for an electron-like ring and might erroneously be taken as the electron-like one. To reduce the background from π^0, the second electron-like ring is looked for this event, the invariant mass is reconstructed, and the condition that it be no less than 105 MeV is imposed. It is also implied that the detected event constituted a quasielastic scattering via charged current and the reconstructed neutrino energy is lower than 1250 MeV. This permits eliminating the high-energy tail in the neutrino

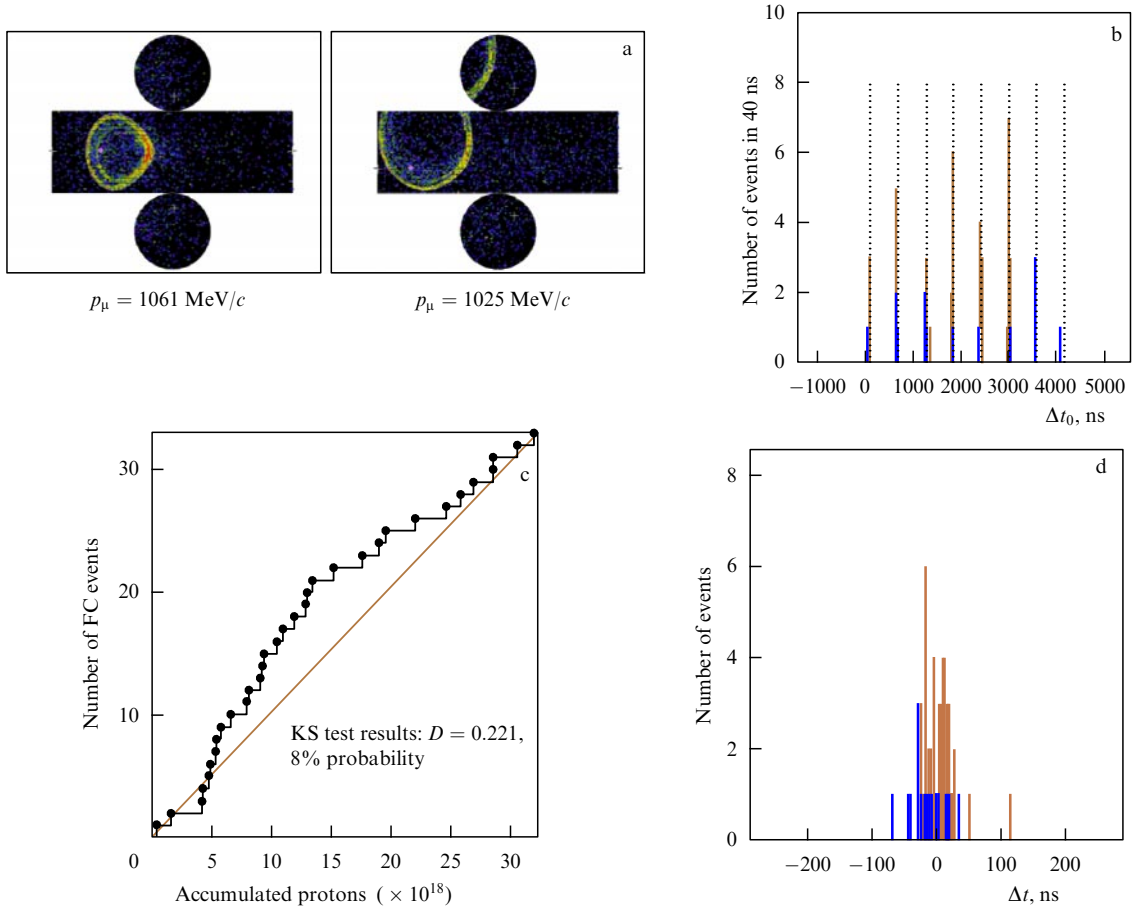

Figure 5. Neutrinos from the J-PARC proton accelerator detected by Super-Kamiokande. (a) Typical muon-like event. (b) Time distribution of recorded events, which corresponds to the accelerator time structure. There are no background events between the accelerator microbunches. (c) Number of events in the detector fiducial volume as a function of the number of protons on the target (FC events — events whose energy is completely absorbed in the Super-Kamiokande inner detector; KS — Kolmogorov–Smirnov criterion). (d) Time distribution of neutrino events ($\sigma = 26$ ns) relative to the center of the accelerator microbunch nearest to the event; Δt is the time interval between the event detection time and the center of the microbunch nearest to the event.

spectra, which contains a large fraction of electron neutrinos. As suggested by Monte Carlo simulations, a substantial lowering of the level of background events (suppression of $\pi^0 \to 2\gamma$ decays by about a factor of 100) is expected under these conditions, and a rather high detection efficiency, about 40%, for the expected signal may be obtained. During the first physics run, one event at Super-Kamiokande was recorded as a candidate for an electron neutrino produced in the detector fiducial volume. In this case, the expected background is estimated to be about 0.28 events.

4. Status of the experiment and immediate plans

The second T2K physical session, which commenced in November 2010, will continue for six months. It is planned to accumulate neutrino events for an integral proton beam power of 150 kW $\times 10^7$ s, which corresponds to $\approx 3 \times 10^{20}$ POT. It is anticipated that a sensitivity of 0.05 (90% CL) to $\sin^2 2\theta_{13}$ will be achieved.

The dependence of experimental sensitivity to θ_{13} (90% CL) on the integral number of protons on the target is plotted in Fig. 6 with the inclusion of possible systematic errors of 5%, 10%, and 20%. The following oscillation parameters were employed for these estimates: $\Delta m^2_{23} \approx 2.4 \times 10^{-3}$ eV^2, $\sin^2 2\theta_{23} = 1.0$, $\Delta m^2_{12} \sim 7.6 \times 10^{-5}$, $\sin^2 2\theta_{12} = 0.87$, and $\delta = 0$, as well as the normal hierarchy of neutrino masses. The dashed arrow shows the ultimate goal of the first experiment stage: $\sin^2 2\theta_{13} = 0.006$ (90% CL) for 8×10^{21} POT, which corresponds to five years of data taking for a proton beam power of 0.75 MW. This sensitivity is expected to be attained within the next two years. In this period, a measurement accuracy of $\delta(\Delta m^2_{23}) \approx 1 \times 10^{-4}$ and $\delta(\sin^2 2\theta_{23}) \approx 0.01$ will be attained in the $\nu_\mu \to \nu_\mu$ process as a result of measurements of event deficit and spectrum shape distortion [29].

Of special note is the paramount importance of the T2K experiment for subsequent investigations with accelerator neutrinos, because the discovery of $\nu_\mu \to \nu_e$ oscillations and a nonzero value of the θ_{13} angle furnish a unique possibility in the quest for *CP* violation in the leptonic sector in long-baseline accelerator experiments. These issues are considered at length in review [30].

In June 2011, the T2K collaboration published the first result [31] of the analysis of the data accumulated in the execution of the experiment from January 2010 to March 11, 2011 (the onset of an earthquake in Japan). Six events were discovered, which were candidates for electron neutrinos. Assuming the absence of $\nu_\mu \to \nu_e$ oscillations (at $\theta_{13} = 0$), the expected number of such events equaled 1.5 ± 0.3. The probability that the six events make up a fluctuation of

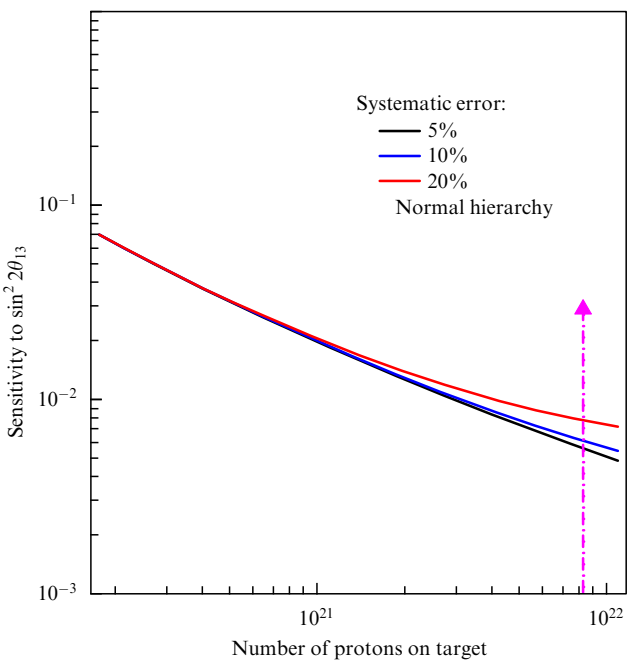

Figure 6. Dependence of the sensitivity to θ_{13} (90% CL) on the number of protons on the target. The three curves correspond to possible systematic errors of 5%, 10%, and 20%. The dashed arrow indicates the anticipated experimental sensitivity ($\sin^2 2\theta_{13} = 0.006$ at 90% CL) for 8.5×10^{21} POT.

background events rather than the result of neutrino oscillations is equal to 0.7%. Therefore, with a probability of 99.3% this result may be interpreted as an indication of $\nu_\mu \to \nu_e$ oscillations. The central value for $\sin^2 2\theta_{13}$ amounts to 0.11 for normal neutrino mass hierarchy, and to 0.14 for inverse hierarchy at $\delta = 0$.

Acknowledgments. This work was supported by the Neutrino Physics Program of the Presidium of the Russian Academy of Sciences, and the Program for Support of Scientific Schools (NSh-65038.2010.2).

References

1. Maki Z, Nakagawa M, Sakata S *Prog. Theor. Phys.* **28** 870 (1962)
2. Fukuda Y et al. (Super-Kamiokande Collab.) *Phys. Rev. Lett.* **81** 1562 (1998)
3. Fukuda Y et al. (Super-Kamiokande Collab.) *Phys. Rev. Lett.* **77** 1683 (1996)
4. Fukuda Y et al. (Super-Kamiokande Collab.) *Phys. Rev. Lett.* **81** 1158 (1998)
5. Abdurashitov J N et al. (SAGE Collab.) *Phys. Lett. B* **328** 234 (1994)
6. Anselmann P et al. (GALLEX Collab.) *Phys. Lett. B* **285** 376 (1992)
7. Ahmad Q R et al. (SNO Collab.) *Phys. Rev. Lett.* **87** 071301 (2001)
8. Ahmad Q R et al. (SNO Collab.) *Phys. Rev. Lett.* **89** 011301 (2002)
9. Eguchi K et al. (KamLAND Collab.) *Phys. Rev. Lett.* **90** 021802 (2003)
10. Ahn M H et al. (K2K Collab.) *Phys. Rev. D* **74** 072003 (2006)
11. Adamson P et al. (MINOS Collab.) *Phys. Rev. Lett.* **101** 131802 (2008); arXiv:0806.2237
12. Apollonio M et al. (CHOOZ Collab.) *Eur. Phys. J. C* **27** 331 (2003)
13. Fogli G L et al. *Prog. Part. Nucl. Phys.* **57** 742 (2006); hep-ph/0506083
14. Barger V, Marfatia D, Whisnant K *Phys. Rev. D* **65** 073023 (2002); hep-ph/0112119
15. Itow Y et al., hep-ex/0106019
16. "T2K ND280 Conceptual Design Report", T2K Internal Document, Version 1.0 (2005)
17. Karlen D (and the ND280 Group of the T2K Collab.) *Nucl. Phys. B Proc. Suppl.* **159** 91 (2006)
18. Kudenko Yu (and Representing the T2K Collab.) *Nucl. Instrum. Meth. Phys. Res. A* **598** 289 (2009)
19. Hayato Y (and the T2K Collab.) *Nucl. Phys. B Proc. Suppl.* **143** 269 (2005)
20. Yamada Y *Nucl. Phys. B Proc. Suppl.* **155** 28 (2006)
21. Yokoyama M et al., physics/0605241
22. Gomi S et al. *Nucl. Instrum. Meth. Phys. Res. A* **581** 427 (2007)
23. Yokoyama M et al. *Nucl. Instrum. Meth. Phys. Res. A* **610** 128 (2009); arXiv:0807.3145
24. Vacheret A et al. *Nucl. Instrum. Meth. Phys. Res. A* **656** 69 (2011); arXiv:1101.1996
25. Mineev O et al. *Nucl. Instrum. Meth. Phys. Res. A* **577** 540 (2007)
26. Izmaylov A et al. *Nucl. Instrum. Meth. Phys. Res. A* **623** 382 (2010); arXiv:0904.4545
27. Fukuda S et al. *Nucl. Instrum. Meth. Phys. Res. A* **501** 418 (2003)
28. Blondel A "Hadron production experiments", in *Neutrino 2010, June 14 – 19, 2010, Athens, Greece*
29. The T2K experiment, http://www.t2k.org
30. Kudenko Yu G *Usp. Fiz. Nauk* **181** 569 (2011) [*Phys. Usp.* **54** 569 2011)]
31. Abe K et al. (T2K Collab.) *Phys. Rev. Lett.* **107** 041801 (2011); arXiv:1106.2822

PACS numbers: **28.60.+s**, **29.20.–c**, 87.56.B–
DOI: 10.3367/UFNe.0181.201109k.1004

Isotope production at the Institute for Nuclear Research, Russian Academy of Sciences: current status and prospects

B L Zhuikov

1. Possibilities of producing radionuclides in intermediate-energy accelerators

It is likely that the idea of producing radionuclides for science and applications appeared when the Institute for Nuclear Research, USSR Academy of Sciences was founded in 1970 and it was decided to construct a linear accelerator of intermediate-energy protons — a meson factory. Beginning from the late 1980s, extensive research and development were performed aimed, first of all, at the construction of a facility for acceleration of heavy ions of radionuclides in a cyclotron specially built for this purpose [1]. It was assumed to produce radionuclides in the proton beam of a linear accelerator and to extract them expressively from irradiated targets. This project was aimed at fundamental studies in the field of nuclear physics. Simultaneously, it was planned to carry out the production of isotopes for medical and technical purposes. A similar program was accepted and is now being realized, for example, at the Legnaro National Laboratories (INFN-LNL) in Italy.

Because of a drastic reduction in financing, the program on heavy ions was not realized, and now the main focus is the

B L Zhuikov Institute for Nuclear Research, Russian Academy of Sciences, Moscow, Russian Federation
E-mail: bz@inr.ru

Uspekhi Fizicheskikh Nauk **181** (9) 1004 – 1011 (2011)
DOI: 10.3367/UFNr.0181.201109k.1004
Translated by M Sapozhnikov; edited by A Radzig